

In Situ Measurement of Breathing Strain and Mechanical Degradation in Organic Electrochromic Polymers

Xiaokang Wang, Luize Scalco de Vasconcelos, Ke Chen, Kuluni Perera, Jianguo Mei,* and Kejie Zhao*



Cite This: *ACS Appl. Mater. Interfaces* 2020, 12, 50889–50895



Read Online

ACCESS |



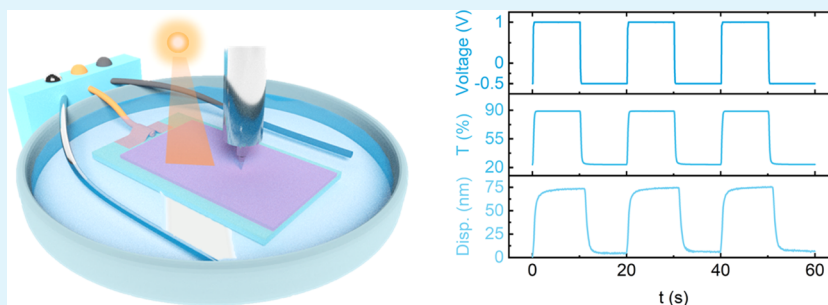
Metrics & More



Article Recommendations



Supporting Information



ABSTRACT: Organic mixed ionic–electronic conductors (OMIECs) are an emerging family of materials crucial in the development of flexible, bio-, and optoelectronics. In electrochromic polymers, the cyclic redox reaction is associated with a mechanical breathing strain, which deforms the OMIECs and degrades the device reliability. We set forth an in situ nanoindentation approach to measure the breathing strain of a poly(3,4-propylenedioxythiophene) (PProDOT) thin film in a customized liquid cell during electrochromic cycles. A breathing volumetric strain of 12–25% is persistent in different sets of electrolytes of various solvents, salts, and salt molarities. The electrochemical conditioning, intermittence time, and cyclic protocol have minor effects on the mechanical response of PProDOT. The mechanical behavior and anion diffusivity measurement further infer the redox kinetics. Heavily cycled PProDOT films show reduced volumetric strain and accumulated mechanical damage of channel cracks and dysfunctional regions of slow and inhomogeneous electrochromic switching. This work is a systematic characterization of mechanical deformation and damage in a model OMIEC and informs the mechanical reliability of organic electrochromic devices.

KEYWORDS: breathing strain, mechanical reliability, electrochromic polymer, in situ experiments, delamination, PProDOT

INTRODUCTION

Organic mixed ionic–electronic conductors (OMIECs), including conducting polymers and small molecules, are the key component for bioelectronics, organic electrochemical transistors, and organic electrochromic devices.^{1–3} Upon doping/dedoping, the physical, chemical, optical, and mechanical properties of OMIECs evolve concurrently. A model organic mixed ionic–electronic conductor, poly(3,4-propylenedioxythiophene) (PProDOT), for instance, switches the color from magenta to the bleached state when it is oxidized (electrochemically doped).^{4,5} To maintain the electroneutrality in electrochromic cycles, anions diffuse into or out from the polymer layer and deform PProDOT.⁶ The repetitive size change of the electrochemically active materials is known as mechanical breathing.⁷ Meanwhile, PProDOT becomes more compliant and softer at the doped state—both elastic modulus and hardness considerably decrease upon oxidation.⁷ The breathing strain was utilized in the design of actuators.⁸ Contrary to actuators such as artificial muscles where large deformation is favored, the OMIEC devices desire small, if not zero, mechanical breathing strain to retain their mechanical reliability over tens of thousands of lifetime cycles.^{9,10} The

mechanical deformation induces a stress field in OMIECs. For example, PProDOT thin-film electrodes expand in volume and are subject to compression upon ionic–electronic doping. The film may wrinkle, buckle, and delaminate from the indium tin oxide (ITO) current collector. During dedoping, the thin film is under tension which drives the formation of channel cracks and reduces material integrity. Both the material degradation and structural disintegration can drastically disrupt the electronic/ionic conducting path and lead to low performance and eventually device failure.⁷

Significant efforts have been devoted to quantifying the mechanical breathing strain in organic electrochemically active materials. For instance, one can measure the length of freestanding films with a load suspended at the bottom of

Received: August 26, 2020

Accepted: October 16, 2020

Published: October 28, 2020



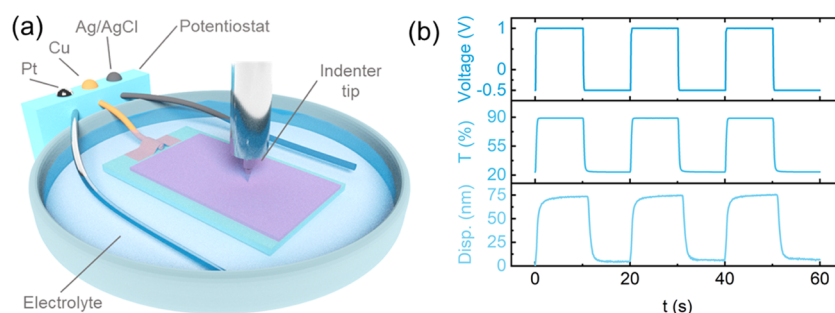


Figure 1. Setup of in situ nanoindentation measurement on the mechanical breathing strain in electrochromic polymers during redox reactions. (a) Sketch of the electrochemical cell and the indenter tip on a PProDOT thin film immersed in the liquid electrolyte. (b) Tip displacement and film transmittance in response to the applied voltage to PProDOT against Ag/AgCl.

the film in an electrolyte.⁸ Alternatively, the films can be stacked in actuators with a layer-by-layer structure.¹¹ The curvature of the actuators was measured via an optical method.¹² For films of submicron thickness, freestanding films are generally too delicate to handle and the curvature of the stressed bilayer is influenced by the substrate. In an earlier work, we set forth a nanoindentation approach to measure the mechanical deformation of electrochromic films during redox reactions in a customized liquid cell.⁷ The volumetric strain of the thin-film electrodes was measured by targeted indentation at the oxidized and reduced states. This technique can be refined to continuously map the local nanoscale deformation of the thin film in situ and over redox cycles.

In this work, we conduct in situ nanoindentation to systematically measure the breathing strain of PProDOT thin-film electrodes in a variety of electrochemical settings. By tracking the thickness change of the thin film using targeted nanoindentation, we show a persistent breathing strain of 12–25% over cycles. The mechanical response of PProDOT in different electrolytes of different solvents, salts, and salt molarities is consistent. The electrochemical conditioning and the intermittence time between cycles have minor effects on the mechanical deformation. Breathing strains under different electrochemical protocols are also compared, which informs the kinetics of redox reactions in PProDOT. We measure the anion diffusivity in PProDOT to validate the experimental observations. In long-term cycling, the thin-film electrodes gradually lose the electrochemical activity and show a reduced mechanical breathing strain. Channel cracks and dysfunctional regimes emerge in the film that degrade the material integrity and deteriorate the device performance.

EXPERIMENTAL SECTION

Film Processing and Characterization. PProDOT was synthesized via direct arylation polymerization.¹³ PProDOT was dissolved in chloroform with a concentration of 40 mg mL⁻¹ and stirred overnight to form a homogeneous solution before use. ITO-coated glass slides were cleaned with ultrasonic in chloroform and then ethanol for 10 min. The PProDOT solution was then spin-coated on ITO-coated glass slides with a spin speed of 800 rpm to form ~480 nm thick films. The absorbance spectra were characterized by an ultraviolet–visible–near-infrared (UV–vis–NIR) spectrometer Cary-5000. The film thickness was measured by both the scratch test and the indentation test described in a previous paper.⁷

In Situ Breathing Strain Measurement. PProDOT film on an ITO-coated glass slide was mounted in a home-made fluid cell.¹⁴ Electrolyte salts LiBF₄, LiClO₄, and LiTFSI were purchased from Sigma-Aldrich. The salts were dissolved into propylene carbonate (PC) solvent (Sigma-Aldrich) and stirred for 12 h to form a

homogeneous liquid electrolyte. 1 M LiPF₆ in PC and 1 M LiPF₆ in ethylene carbonate and diethyl carbonate (EC/DEC, v/v = 50:50) were purchased from Sigma-Aldrich. Using Pt wire as the counter electrode and home-made Ag/AgCl wire¹⁵ as the reference electrode, the electrochemical test was conducted using VersaSTAT 3 station. Instrumented nanoindentation (G200 Nanoindenter, KLA) was used to track the surface of the film using a very gentle contact force (<1 μN).

RESULTS AND DISCUSSION

Even though the volumetric change of the electrodes during redox reactions is now well recognized, in situ characterization of such mechanical breathing remains a challenge. Here, we use instrumented nanoindentation to track the motion of the top surface of thin-film electrodes during redox cycles, as shown in Figure 1a. The images of the experimental setup are shown in Figure S1. A PProDOT film deposited on an ITO-coated glass slide is mounted firmly on the fluid cell and serves as the working electrode.¹⁴ The electrochemical cell also consists of a reference electrode (Ag/AgCl wire) and a counter electrode (Pt wire). The indenter tip travels vertically on top of the film. When the surface is detected, the tip stays in contact with the sample with a gentle contact force. The penetration of the tip into the film is negligible at the applied force. An electrical potential (1 V against Ag/AgCl) is applied to trigger the electrochromic reaction. The redox reaction largely alters the chemical, physical, and mechanical properties of the film electrode. Under a positive voltage, the neutral PProDOT molecules are electrochemically doped.¹⁶ As a result, the absorbance in the visible spectrum diminishes, and the transmittance increases⁵ (Figure 1b). Simultaneously, counterions are injected into the film to maintain electrical neutrality. The mass transport is accommodated by an expansion of the film. Consequently, the tip is pushed upwards with the rising surface. Next, the applied potential is held at 1 V for 10 s. The holding time is long enough for the ionic–electronic doping to complete, as indicated by the plateau of both the transmittance and the tip displacement. Upon applying a negative potential (−0.2 V), the film is reduced to the neutral state with low transmittance. The counterions are ejected and the nanoindenter tip follows the descending surface. The tip displacement δd equals the change in the thickness of the thin film δh . Using the thickness of the pristine film h_0 , the volumetric strain of the film during the redox reaction is calculated as $\epsilon_v = \delta d / h_0$. To minimize the effect of material fatigue and irreversible tip penetration, the measurement at a single location is limited to 15 cycles.

The volumetric strain originates from the injection of counterions, which is inherent to the redox reaction. To

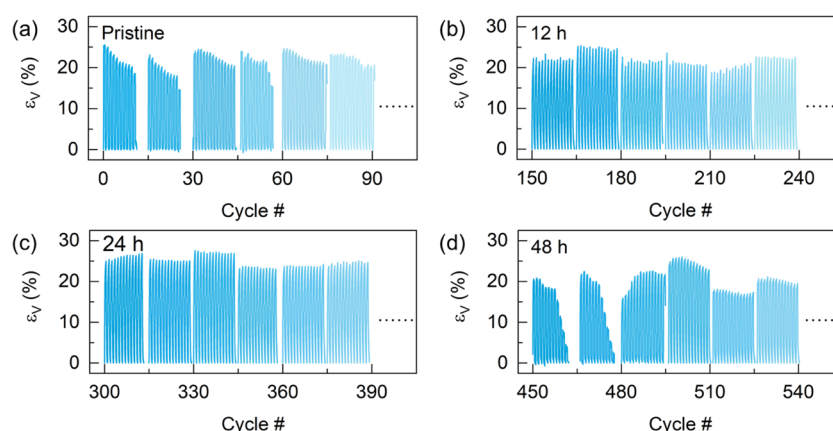


Figure 2. Effect of electrochemical conditioning and intermittence on the breathing strain. Different shades denote the strains measured at different locations to avoid the fatigue of the material. The indentation locations are randomly selected within the film. (a) Volumetric strain in PProDOT during the initial 90 cycles; (b–d) evolution of the volumetric strain with an intermittence of 12, 24, and 48 h in the following cycles, respectively.

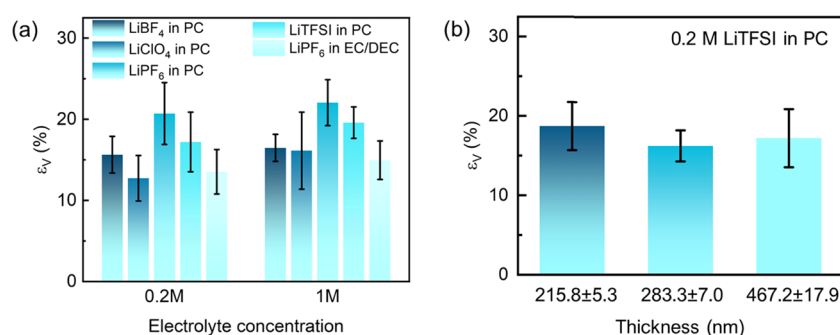


Figure 3. Mechanical breathing strain in the PProDOT thin film. (a) Effect of the electrolyte. (b) Effect of the film thickness.

explore the effect of electrochemical conditioning and intermittence time between cycles on the mechanical response, we measure the volumetric strain of the film from the pristine state up to 600 cycles in the liquid electrolyte of 1 M LiPF₆ in PC, and with an intermittence time of 12, 24, and 48 h between every 150 cycles. Figure 2 summarizes the results. The different batches of results of different shades represent the measurements at different locations. The breathing strain is consistent for all of the test cases, and the range is 20–22% with a little statistical variation. We do not observe any substantial effect of electrochemical conditioning in the first few cycles or after the PProDOT film is set at rest and then reactivated after 12, 24, and 48 h—the mechanical response is nearly instantaneous upon the redox reaction and remains steady over cycles. For the test after 450 cycles, the strain appears slightly nonuniform at different locations. This may be caused by the degradation of the film, which will be discussed in detail in a later section. The results confirm that the mechanical breathing strain is inherent to the electrochemical cycle. We note that the volumetric strain measured in the early cycles is slightly smaller than the previous measurement using the scratch test and targeted indentation test.⁷ This discrepancy comes from the irreversible deformation of the film by tip penetration during the long time (>300 s) holding, as shown in the raw displacement in Figure S2.

Anions play a critical role in electrochromic reactions. To evaluate the effects of anions and solvents, we compare the volumetric strain of PProDOT in different sets of electrolytes of various solvents, salts, and salts concentrations. Two solvents (PC and EC/DEC), four salts (LiBF₄, LiClO₄,

LiPF₆, and LiTFSI), two salt molarities (0.2 and 1 M), and their combinations are tested. Figure 3a summarizes the results measured in two different samples for each setting. Each sample is measured at ~10 different locations with over 100 cycles in total. Overall, the volumetric strain is in the range from 12.7% (0.2 M LiClO₄ in PC) to 22.1% (1 M LiPF₆ in PC). The mechanical deformation of PProDOT in the liquid electrolyte of 1 M salt is generally larger than the counterpart of 0.2 M. With a given salt concentration and solvent, the breathing strain is in the following order $\epsilon_{V|LiPF_6} > \epsilon_{V|LiTFSI} > \epsilon_{V|LiBF_4} > \epsilon_{V|LiClO_4}$. The correlation between the mechanical response of the film and the choice of the anion is unclear in this writing. The breathing strain is presumably determined by the number of injected anions and solvent molecules, the size of the anions, and the morphological rearrangement of the polymer after ionic–electronic doping.^{17–19} Current results demonstrate that the mechanical breathing strain in electrochromic polymers can be potentially mitigated by the selection of the electrolyte. The fundamental understanding behind this observation, nevertheless, warrants a future detailed study at the molecular level. In addition, to study the thickness dependency of mechanical behavior, we measure the breathing strain in PProDOT films of three different thicknesses. The films are processed by different solution concentrations (20, 30, 40 mg mL^{−1}). With a spin speed of 800 rounds per minute, the thickness of the films is 215.8 ± 5.3, 283.2 ± 7.0, and 467.2 ± 17.9 nm, respectively. The results of the breathing strain of the films with the electrolyte 0.2 M LiTFSI in PC are 18.7%, 16.2%, 17.2%, respectively, as shown in Figure 3b.

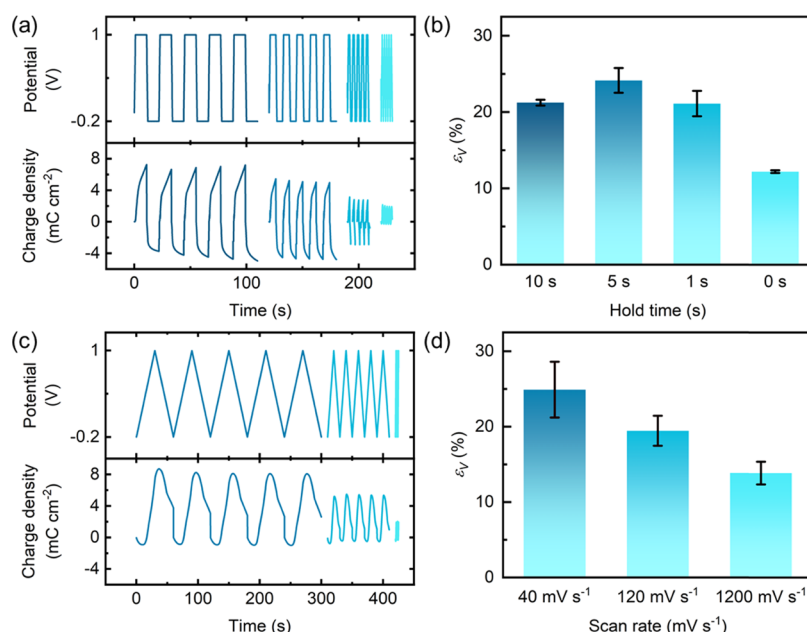


Figure 4. Breathing strain of PProDOT under various potential conditions. (a) Voltage and charge density profiles during cyclic voltammetry with a hold time of 10, 5, 1, and 0 s. (b) Mechanical breathing strain under different hold times at the peak voltage. (c) Voltage and charge density profiles during cyclic voltammetry using a scan rate of 40, 120, and 1200 mV s⁻¹. (d) Breathing strain for the different sweeping rates.

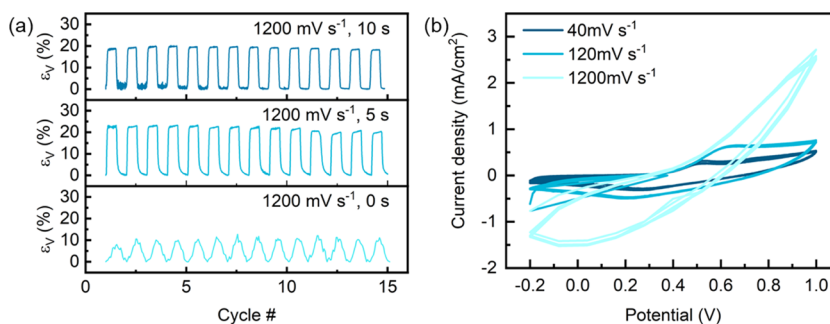


Figure 5. Kinetics of the redox reaction. (a) Breathing strain of PProDOT for different hold times at the peak voltage. (b) Cyclic voltammograms of the PProDOT film at the scan rate of 40, 120, and 1200 mV s⁻¹.

We further evaluate the effect of the cyclic protocol by prescribing two different potential profiles. In the first measurement, a chronoamperometry test is performed with a stepwise potential as shown in Figure 4a. After ramping up to the peak potential (1 V for oxidation and -0.2 V for reduction) in 1 s, the peak voltages are held for 10, 5, 1, and 0 s (no holding), respectively. The hold time at the redox peak potentials, the electron and anion transport, and the structural relaxation (molecular rearrangement upon doping/dedoping) of the polymer constitute the time scales that influence the mechanical response of the thin film—when the hold time is sufficiently long, the ion injection and the local structural changes reach a steady state and so does the volumetric strain. On the other hand, when the hold time is short, the mechanical response of the polymer undergoes a transient state. The lower panel in Figure 4a shows the charge density at different hold times. As the hold time reduces from 10 to 0 s, the charge density steadily decreases from 7 to 2 mC cm⁻². Figures 4b and S3 show the breathing strain of PProDOT in the electrolyte of 0.2 M LiTFSI in PC for ~100 cycles. The volumetric strain for the hold times of 1, 5, and 10 s reaches a steady-state value of 21–24%, which indicates that 1 s is likely sufficient for ion injection into the polymer. The slightly

smaller deformation at the hold time 10 s is probably due to the creep of the material that partially relaxes the volumetric strain. With 0 s hold time at the peak voltage, the breathing strain is only about 12% because of the considerably smaller charge density involved in the redox reaction. The relationship between the charge density and the mechanical strain calls for optimum design in organic electrochromic devices—while the optical contrast and high coloration efficiency often require a complete electrochromic reaction, deep charging/discharging also induces large deformation of the electrodes to accommodate the ion-electron injection. The repetitive large deformation can severely reduce the mechanical reliability of the device. Future design of OMIECs should be focused on minimizing the mechanical breathing strain in the active materials while retaining the desired optoelectronic performance.

In the second test, we conduct cyclic voltammetry at different scan rates, as shown in Figure 4c. The volumetric strains are measured under different scan rates of 40, 120, and 1200 mV s⁻¹. The corresponding charge densities are 8, 5, and 2 mC cm⁻², respectively. As shown in Figures 4d and S4, the breathing strain is 25%, 19%, and 14%, respectively. With the increase of the scan rate, both the charge density and the

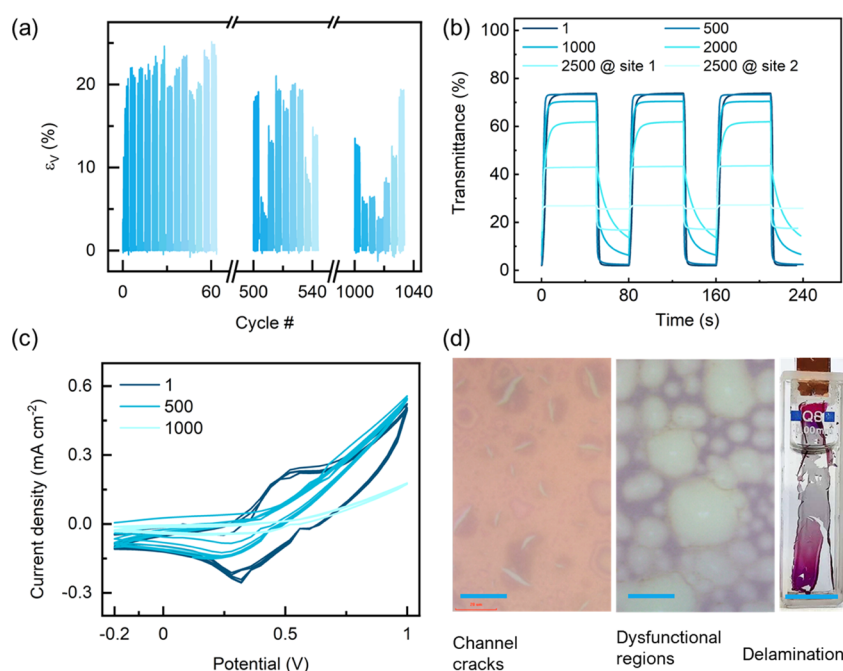


Figure 6. Mechanical degradation of the PProDOT film. (a) Breathing strain, (b) optical transmittance, and (c) cyclic voltammetry for heavily cycled films. (d) Optical images showing channel cracks (scale bar 20 μm), dysfunctional regions (scale bar 100 μm), and film delamination (scale bar 1 cm) in PProDOT.

volumetric strain drop significantly. This result suggests that the anion diffusion is likely the rate-limiting process during fast scanning and the incomplete redox process likely reduces the overall mechanical deformation in PProDOT.

The mechanical response of the polymer informs the kinetics of the electrochromic reaction. As shown in Figure 5a, the volumetric strain evolves as a step function for the 10 and 5 s hold times, suggesting that the kinetic process is complete. For the 0 s hold time, the kinetic process is yet to complete, and the strain profile exhibits a triangular shape without plateau. In the case of 5 s hold time, the oxidation process (increasing volume) has a sharp transition while the reduction (decreasing volume) undergoes a gradual transition. This is evidence that the oxidation process proceeds much faster than the reduction reaction. This asymmetric behavior is analogous to the lithiation reaction in amorphous Si electrodes for Li-ion batteries—Li insertion in Si takes place at a much faster rate than delithiation.²⁰ In the oxidation process, the conductivity of the polymer increases in favor of fast electronic charge transfer, and the structure also becomes more conductive to facilitate ionic transport.²¹ In the reduction process when anions are extracted, the electronic/ionic conductivity of the polymer decreases, which impedes the dedoping reaction. The composition-dependent electronic conductivity and ionic diffusivity can create an asymmetric rate capability of doping and dedoping and potentially traps the counterions in the polymers, which reduces the optical contrast of electrochromic devices over long-term cycles.

We use the Randles–Sevcik equation,²² $i_p = 2.69 \times 10^5 n^{3/2} A D^{1/2} C \nu^{1/2}$, to determine the anion diffusivity, where i_p is the peak current in ampere, n is the number of electrons transferred in the redox reaction (assuming 1 for single-charged polarons in PProDOT), A is the area of the electrode in cm^2 , D is the diffusivity in $\text{cm}^2 \text{s}^{-1}$, C is the anion concentration in mol cm^{-3} , and ν is the scan rate in V s^{-1} . Here, we use the PProDOT thin-film sample of the area of 0.4

cm^2 and in the electrolyte 0.2 M LiTFSI in PC. The diffusivity is determined as 2.5×10^9 , 5.0×10^9 , and $6.4 \times 10^8 \text{ cm}^2 \text{s}^{-1}$ for the scan rate of 40, 120, and 1200 mV s^{-1} , respectively. Using the film thickness of 480 nm, the time scale of diffusion²³ is $t \sim L^2/D = 1.01, 0.50, \text{ and } 0.04 \text{ s}$, respectively, for the three scan rates. This calculation is consistent with the observation in Figure 4b, where 1 s is likely sufficient for anion diffusion and therefore the mechanical response reaches a steady state for the hold time longer than 1 s. We also note that the diffusion time of anion is less than or on the same order of magnitude of the general voltage ramping time in electrochromic devices. The time scale for the structural relaxation (material creep), on the other hand, is usually much longer than that for ionic/electronic transport. The electrochemically stimulated conformational relaxation model²⁴ demonstrates that structural relaxation in polymers occurs concomitantly with the ionic/electronic transport. A slow structural relaxation might impede the diffusion of the counterions and acts as a rate-limiting factor in the redox reactions. To expedite the switching speed, new synthesis and processing schemes should be applied to achieve a more porous molecular network that facilitates structure relaxation and ionic transport.

The mechanical breathing causes degradation of the material integrity and structural stability as the redox reaction proceeds. We monitor the volumetric strain of PProDOT at randomly selected sites from the pristine state up to 1000 cycles. Figure 6a shows the breathing strain profile. For the as-synthesized thin film, the mechanical deformation is $\sim 20\%$ in the early cycles. After 500 cycles, the volumetric strain at some sites decreased to below 10%. Over 1000 cycles, the breathing strain for nearly all of the measured locations has significantly dropped. The heterogeneous degradation in the film also manifests as the transmittance drops as measured from a separate film under the same cyclic protocol (Figures 6b and S5). The difference of the transmittance in the colored and bleached states, ΔT , is over 70% in the pristine sample and

decreases drastically as the cycle number goes beyond 500. Measurements after 2500 cycles at two different sites show that ΔT is 5–30%. Optical density and coloration efficiency also show the same decreasing trend (the different coloration efficiencies measured after 2500 cycles at the two sites are due to the heterogeneous damage of the PProDOT film), as listed in Table S1. The locally resolved reduction of the mechanical response and the optical performance is consistent with the loss of the electrochemical activity as shown in the cyclic voltammetry (Figure 6c). The oxidation onset voltage for the pristine film is around 0.3 V against Ag/AgCl. The current peak at 0.5 V corresponds to the oxidation of PProDOT. After 500 cycles, the peak at 0.5 V disappeared. After 1000 cycles, the current density significantly decreased. All of the above observations are evidence of material degradation and structural damage for the heavily cycled films. As shown in Figure 6d, randomly distributed channel cracks of length ~ 10 μm , dysfunctional regions of radii ~ 100 μm , and large-scale film delamination at the size of ~ 1 cm are observed after hundreds of cycles. The channel cracks evolve as a result of the tensile stress inside the film during the reduction reaction. As shown in the Supporting Information Movie 1, the film swells, and the channel cracks close in the oxidation process. During reduction, the film shrinks in volume, and the channel cracks reopen due to the tensile stress.⁷ The dysfunctional regions are induced mostly likely due to the interfacial delamination between the PProDOT film and the ITO substrate, which destroys the electronic transport path. Supporting Information Movie 2 shows the dynamic process. Although the image quality is limited by the optical microscope, it is clear that the intact regions remain functional and can change color immediately upon the applied potential (vertical electronic conduction), while the reactions proceed slowly into the bubblelike dysfunctional regions through the lateral electronic conduction path. As the mechanical damage evolves, the film delamination from the ITO current collector emerges, which eventually destruct the electrode. Possible solutions to mitigate the mechanical degradation in organic electrochromic devices are proposed in the previous literature,^{7,25} including (1) synthesizing materials with low breathing strain and high cohesion strength; (2) toughening the interface chemically, physically, and/or mechanically; and (3) developing a flexible and mechanically compatible substrate.

CONCLUSIONS

This study focuses on the mechanical breathing strain and the consequent material degradation of an organic electrochromic polymer under a variety of redox conditions. We measure the real-time evolution of the mechanical deformation in a PProDOT thin film in the liquid cell using in situ nanoindentation. The mechanical response is nearly instantaneous upon the redox reaction. The electrochemical conditioning and the intermittence time between each batch of cycles have negligible effects on the mechanical response of the polymer. We test multiple electrolytes of different solvents, salts, and salt concentrations. The volumetric strain of PProDOT is within the range of 12–25%. The mechanical behavior of the electrochromic polymer informs the kinetics of the redox reaction. We use an electroanalytical approach to measure the anion diffusivity to corroborate the mechanical measurement. The rate performance at different hold times suggests that oxidation in PProDOT proceeds faster than reduction. This asymmetric rate capability can potentially trap

counterions in the fast switching and reduce the optical contrast of devices in long-term cycles. The mechanical breathing causes severe material damage and structural failure in organic electrochromic devices. Channel cracks and interfacial delamination emerge as the major modes of mechanical degradation, which significantly reduce the electrochemical activity and optical performance in PProDOT.

ASSOCIATED CONTENT

Supporting Information

The Supporting Information is available free of charge at <https://pubs.acs.org/doi/10.1021/acsami.0c15390>.

Raw displacement of indenter tip; breathing strain of the PProDOT film for different peak voltage hold times and scan rates; absorbance spectra; coloration efficiency calculation (PDF)

Evolution of channel cracks during redox reactions. (MP4)

Evolution of dysfunctional area in redox reaction. (MP4)

AUTHOR INFORMATION

Corresponding Authors

Jianguo Mei – Department of Chemistry, Purdue University, West Lafayette, Indiana 47907, United States; orcid.org/0000-0002-5743-2715; Email: jgmei@purdue.edu

Kejie Zhao – School of Mechanical Engineering, Purdue University, West Lafayette, Indiana 47907, United States; orcid.org/0000-0001-5030-7412; Email: kjzhao@purdue.edu

Authors

Xiaokang Wang – School of Mechanical Engineering, Purdue University, West Lafayette, Indiana 47907, United States

Luize Scalco de Vasconcelos – School of Mechanical Engineering, Purdue University, West Lafayette, Indiana 47907, United States

Ke Chen – Department of Chemistry, Purdue University, West Lafayette, Indiana 47907, United States

Kuluni Perera – Department of Chemistry, Purdue University, West Lafayette, Indiana 47907, United States

Complete contact information is available at: <https://pubs.acs.org/doi/10.1021/acsami.0c15390>

Author Contributions

The manuscript was written through the contributions of all authors. All authors have approved the final version of the manuscript.

Notes

The authors declare no competing financial interest. J.M. is a co-founder of Ambilight Inc.

ACKNOWLEDGMENTS

K.Z., X.W., and L.S.V. acknowledge the support by the National Science Foundation through the grant CMMI-1726392. J.M. is grateful for the financial support from Ambilight Inc.

REFERENCES

- (1) Rivnay, J.; Inal, S.; Salleo, A.; Owens, R. M.; Berggren, M.; Malliaras, G. G. Organic Electrochemical Transistors. *Nat. Rev. Mater.* 2018, 3, 1–14.

- (2) Paulsen, B. D.; Tybrandt, K.; Stavrinidou, E.; Rivnay, J. Organic Mixed Ionic–Electronic Conductors. *Nat. Mater.* **2020**, *19*, 13–26.
- (3) Li, X.; Perera, K.; He, J.; Gumyusenge, A.; Mei, J. Solution-Processable Electrochromic Materials and Devices: Roadblocks and Strategies towards Large-Scale Applications. *J. Mater. Chem. C* **2019**, *7*, 12761–12789.
- (4) He, J.; You, L.; Mei, J. Self-Bleaching Behaviors in Black-to-Transmissive Electrochromic Polymer Thin Films. *ACS Appl. Mater. Interfaces* **2017**, *9*, 34122–34130.
- (5) Kumar, A.; Welsh, D. M.; Morvant, M. C.; Piroux, F.; Abboud, K. A.; Reynolds, J. R. Conducting Poly(3,4-Alkylenedioxythiophene) Derivatives as Fast Electrochromics with High-Contrast Ratios. *Chem. Mater.* **1998**, *10*, 896–902.
- (6) Reynolds, J. R.; Pyo, M.; Qiu, Y.-J. Cation and Anion Dominated Ion Transport during Electrochemical Switching of Polypyrrole Controlled by Polymer-Ion Interactions. *Synth. Met.* **1993**, *55*, 1388–1395.
- (7) Wang, X.; Chen, K.; de Vasconcelos, L. S.; He, J.; Shin, Y. C.; Mei, J.; Zhao, K. Mechanical Breathing in Organic Electrochromics. *Nat. Commun.* **2020**, *11*, No. 211.
- (8) Hara, S.; Zama, T.; Takashima, W.; Kaneto, K. TFSI-Doped Polypyrrole Actuator with 26% Strain. *J. Mater. Chem.* **2004**, *14*, 1516–1517.
- (9) Melling, D.; Martinez, J. G.; Jager, E. W. H. Conjugated Polymer Actuators and Devices: Progress and Opportunities. *Adv. Mater.* **2019**, *31*, No. 1808210.
- (10) Liang, Y.; Ernst, M.; Brings, F.; Kireev, D.; Maybeck, V.; Offenhäusser, A.; Mayer, D. High Performance Flexible Organic Electrochemical Transistors for Monitoring Cardiac Action Potential. *Adv. Healthcare Mater.* **2018**, *7*, No. 1800304.
- (11) Maziz, A.; Plesse, C.; Soyer, C.; Chevrot, C.; Teyssié, D.; Cattan, E.; Vidal, F. Demonstrating KHz Frequency Actuation for Conducting Polymer Microactuators. *Adv. Funct. Mater.* **2014**, *24*, 4851–4859.
- (12) Sen, S.; Kim, S. Y.; Palmore, L. R.; Jin, S.; Jadhav, N.; Chason, E.; Palmore, G. T. R. In Situ Measurement of Voltage-Induced Stress in Conducting Polymers with Redox-Active Dopants. *ACS Appl. Mater. Interfaces* **2016**, *8*, 24168–24176.
- (13) Estrada, L. A.; Deininger, J. J.; Kamenov, G. D.; Reynolds, J. R. Direct (Hetero)Arylation Polymerization: An Effective Route to 3,4-Propylenedioxythiophene-Based Polymers with Low Residual Metal Content. *ACS Macro Lett.* **2013**, *2*, 869–873.
- (14) de Vasconcelos, L. S.; Xu, R.; Zhao, K. Operando Nano-indentation: A New Platform to Measure the Mechanical Properties of Electrodes during Electrochemical Reactions. *J. Electrochem. Soc.* **2017**, *164*, A3840–A3847.
- (15) da Silva, E. T. S. G.; Miserere, S.; Kubota, L. T.; Merkoçi, A. Simple On-Plastic/Paper Inkjet-Printed Solid-State Ag/AgCl Pseudoreference Electrode. *Anal. Chem.* **2014**, *86*, 10531–10534.
- (16) Neo, W. T.; Chua, M. H.; Xu, J. W. Fundamentals of Electrochromic Materials and Devices. In *Electrochromic Smart Materials: Fabrication and Applications*; Smart Materials Series; The Royal Society of Chemistry: Croydon, 2019; pp 22–50.
- (17) Cendra, C.; Giovannitti, A.; Savva, A.; Venkatraman, V.; McCulloch, I.; Salleo, A.; Inal, S.; Rivnay, J. Role of the Anion on the Transport and Structure of Organic Mixed Conductors. *Adv. Funct. Mater.* **2019**, *29*, No. 1807034.
- (18) Modarresi, M.; Mehandezhiyski, A.; Fahlman, M.; Tybrandt, K.; Zozoulenko, I. Microscopic Understanding of the Granular Structure and the Swelling of PEDOT: PSS. *Macromolecules* **2020**, *53*, 6267–6278.
- (19) Savva, A.; Cendra, C.; Giugni, A.; Torre, B.; Surgailis, J.; Ohayon, D.; Giovannitti, A.; McCulloch, I.; Di Fabrizio, E.; Salleo, A.; Rivnay, J.; Inal, S. Influence of Water on the Performance of Organic Electrochemical Transistors. *Chem. Mater.* **2019**, *31*, 927–937.
- (20) de Vasconcelos, L. S.; Xu, R.; Zhao, K. Quantitative Spatiotemporal Li Profiling Using Nanoindentation. *J. Mech. Phys. Solids* **2020**, *144*, No. 104102.
- (21) Flagg, L. Q.; Giridharagopal, R.; Guo, J.; Ginger, D. S. Anion-Dependent Doping and Charge Transport in Organic Electrochemical Transistors. *Chem. Mater.* **2018**, *30*, 5380–5389.
- (22) Bard, A. J. *Electrochemical Methods: Fundamentals and Applications*, 2nd ed.; Wiley: New York, 2001.
- (23) Balluffi, R. W.; Allen, S. M.; Carter, W. C. Diffusion in Noncrystalline Materials. In *Kinetics of Materials*; John Wiley & Sons, Ltd, 2005; pp 229–249.
- (24) Otero, T. F.; Grande, H.; Rodríguez, J. A New Model for Electrochemical Oxidation of Polypyrrole under Conformational Relaxation Control. *J. Electroanal. Chem.* **1995**, *394*, 211–216.
- (25) Wei, B.; Liu, J.; Ouyang, L.; Martin, D. C. POSS-ProDOT crosslinking of PEDOT. *J. Mater. Chem. B* **2017**, *5*, 5019–5026.